

Concepts of medium-range (1–3 days) geomagnetic forecasting

Hans Gleisner *, Jürgen Watermann

Danish Meteorological Institute, Atmosphere Space Research Division, Lyngbyvej 100, Copenhagen, Denmark

Received 3 October 2004; received in revised form 6 September 2005; accepted 10 October 2005

Abstract

To make deterministic medium-range (1 to 3 days ahead) forecasts would require prediction of the detailed near-Earth solar-wind conditions – including the out-of-ecliptic interplanetary magnetic field component – days ahead from remote observations of the inner heliosphere. This is, however, not feasible and will not be in the foreseeable future. Nevertheless, important steps can be taken towards a more physics based approach to geomagnetic forecasting. In this report from an ongoing study within the ESA Space Weather Applications Pilot Project, we discuss presently used concepts and new ideas for fully automatic provision of geomagnetic activity forecasts hours to days ahead. Observations of eruptive events on the Sun are nowadays routinely used as predictors of strong ($Dst < -100$ nT) magnetic storms, but these predictions are still hampered by many false alarms. We here suggest to use the flux of >10 MeV solar energetic particles as a discriminator of potentially geoeffective halo coronal mass ejections, substantially reducing the false alarm rate. We also describe how low speed/high speed solar-wind stream interfaces can be automatically detected in currently available solar-wind models, and point out that, in the absence of eruptive events on the Sun, these may be used as predictors of moderate ($Dst < -50$ nT) magnetic storms, effectively introducing a deterministic element into the mainly probabilistic forecast schemes.
© 2005 COSPAR. Published by Elsevier Ltd. All rights reserved.

Keywords: Geomagnetic forecasting; Space weather; Magnetic storm; Coronal mass ejection; Solar-wind model

1. Introduction

From the Sun–Earth libration point L_1 it takes the solar-wind plasma about an hour to reach the Earth, the exact travel time depending on the solar-wind speed. Since the ACE and SOHO spacecraft began real-time solar-wind monitoring from this vantage point in space, a number of empirical models relating geomagnetic activity to the solar-wind conditions have been converted to operational use. Most of these models predict a geomagnetic index, e.g., Dst , AE , Kp , or locally observed geomagnetic disturbances (e.g., Gleisner and Lundstedt, 2001; O’Brien and McPherron, 2000; Valdivia et al., 1999) from a time series of solar-wind data. Even though the models do not have an intrinsic forecasting capability, the finite solar-wind travel time from L_1 to the Earth nevertheless allow forecasts to be made with a lead time of about an hour. Hence, *short-*

range geomagnetic forecasts (an hour ahead) have become a reality.

These models are *deterministic* in the sense that for a given input, a given output is produced. To use such models beyond a lead time of one hour would require either monitoring of the solar-wind further upstream in the solar-wind, or the use of models to predict the near-Earth solar-wind from remote observations of processes taking place close to the Sun. To make deterministic *medium-range* forecasts (1–3 days ahead) of geomagnetic disturbances, the out-of-ecliptic interplanetary magnetic field (IMF) component B_Z would have to be predicted. Due to the small spatial and temporal scales of typical B_Z variations, this is not possible and will not be in the foreseeable future, except for the rare occasions when the spatial scales of B_Z are unusually large (Zhao and Hoeksema, 1997).

This fundamental limitation is the reason why medium-range geomagnetic forecasts have to be based on *probabilistic* methods (Joselyn, 1995; McPherron and Siscoe, 2004). It is well known that the geomagnetic disturbance field

* Corresponding author. Tel.: +45 39 157 484.
E-mail address: hgl@dmi.dk (H. Gleisner).

have a strong tendency to persistent and recurrent behaviour (Bartels, 1932; Sargent, 1986). In combination with solar-cycle, seasonal, or diurnal climatologies, this property can be utilized for predictive purposes (e.g., Detman, 1996; Thomson, 1996). The accuracy of such statistics based forecasts is, however, too low for many practical applications. The most serious shortcoming is perhaps the lack of skill for predicting strong disturbances of a non-recurrent nature, which means that most strong storms will be missed by these methods.

The present availability of a wide range of solar observations, rapidly processed and dispersed to the user community in near-real time, allow us to go beyond statistics based forecasting. As shown in Fig. 1, the solar sources of geomagnetic activity can schematically be separated into transient *eruptive events* and quasi-static *recurrent structures* co-rotating with the Sun. Observations of eruptive events on the Sun are nowadays routinely used as predictors of magnetic storms, even though these predictions still are hampered by many false alarms. In Section 2, we describe the role of solar eruptive events in geomagnetic forecasting and suggest a potential role for observations of solar energetic particles (SEPs). In the absence of eruptive events on the Sun, observations of solar magnetic fields and the soft X-ray distribution across the solar disk are often used to infer the probable solar-wind conditions over the next few days. In Section 3, we discuss how solar-wind models may be used for this purpose, and how a fully automatic extraction of relevant information could be accomplished. We note that this use of solar-wind models actually introduce a deterministic element into the mainly probabilistic forecast schemes. By combining the two

modes of forecast – that based on transient eruptive events and that based on quasi-static recurrent structures – into an automatically operating forecast scheme, we wish to be able to state whether moderate ($Dst \leq -50$ nT) or strong ($Dst \leq -100$ nT) geomagnetic storms will occur within a specified time period beginning with the probable arrival at Earth of a geoeffective solar-wind structure.

The study described in this paper has been done at the Danish Meteorological Institute within the ESA Space Weather Applications Pilot Project.

2. Solar eruptive events

The strongest geomagnetic disturbances, and many moderate disturbances, do not exhibit a recurrent pattern. Instead, they are primarily associated with transient eruptive events on the Sun. A wealth of observational data presently gives us prompt information of such events, but utilization of these data is not straightforward: solar observations only give an incomplete picture of the associated interplanetary disturbance, and the interpretation in terms of an expected geomagnetic disturbance is hampered by much uncertainty. Nevertheless, observations of solar eruptive events is currently the single most important means to make accurate medium-range geomagnetic forecasts.

2.1. Observations and real time data

Transient eruptive events on the Sun manifest themselves across the electromagnetic spectrum, ranging from bursts of enhanced radio flux to sudden order-of-magnitude increases of solar UV and X-ray fluxes. Sweep-frequency radio bursts indicate the propagation of shock waves in the low solar corona, while enhanced fluxes of energetic particles may indicate the presence of shocks in interplanetary space.

Coronal mass ejections (CMEs) are routinely detected from white-light coronagraph images obtained by the LASCO instrument onboard the SOHO spacecraft, which also carry the EIT instrument by which the nature and location of associated EUV activity in the low solar corona is disclosed. Through an effort by the LASCO team at the Naval Research Laboratories, data on halo CMEs are rapidly dispersed to the user community to give an early warning of possible space weather disturbances (St. Cyr et al., 2000). Information extracted from LASCO images are also provided by the Solar Influences Data Center (SIDC) in Belgium (Berghmans et al., 2002). The CME data from SIDC are obtained through a fully automatic procedure and appear in a less processed form than the NRL data, which are partially based on the subjective judgements of a human forecaster.

High fluxes of solar energetic particles (SEPs) lasting for more than a few hours are known to be generated primarily by strong shock waves propagating in the interplanetary medium. Such SEP events exhibit a close

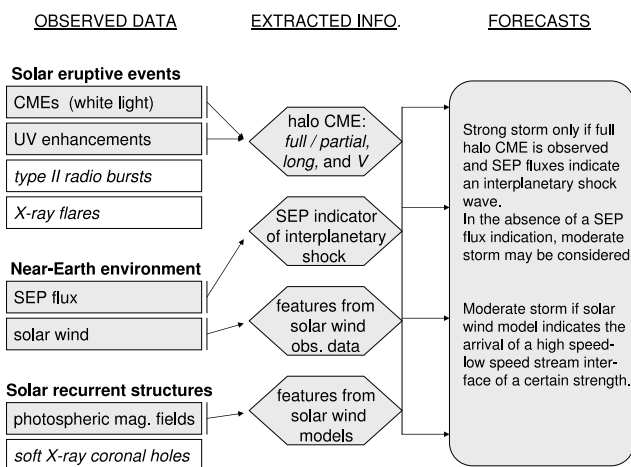


Fig. 1. CMEs and related *solar eruptive events* are the predominant indicators of strong geomagnetic storms, while SEP flux enhancements may indicate if a CME is potentially geoeffective. In the absence of eruptive events on the Sun, quasi-static *solar recurrent structures* co-rotating with the Sun generate geoeffective solar-wind disturbances. These may be detected from features in solar-wind models based on observations of the large-scale solar magnetic fields. Handling the observed data, extracting the relevant information, and combining it properly is essential to make medium-range geomagnetic forecasts.

association with CMEs, particularly those having high velocities. The SEP fluxes are observed by instruments onboard the GOES geostationary satellites and are distributed in near-real time through NOAA's Space Environment Center in Boulder.

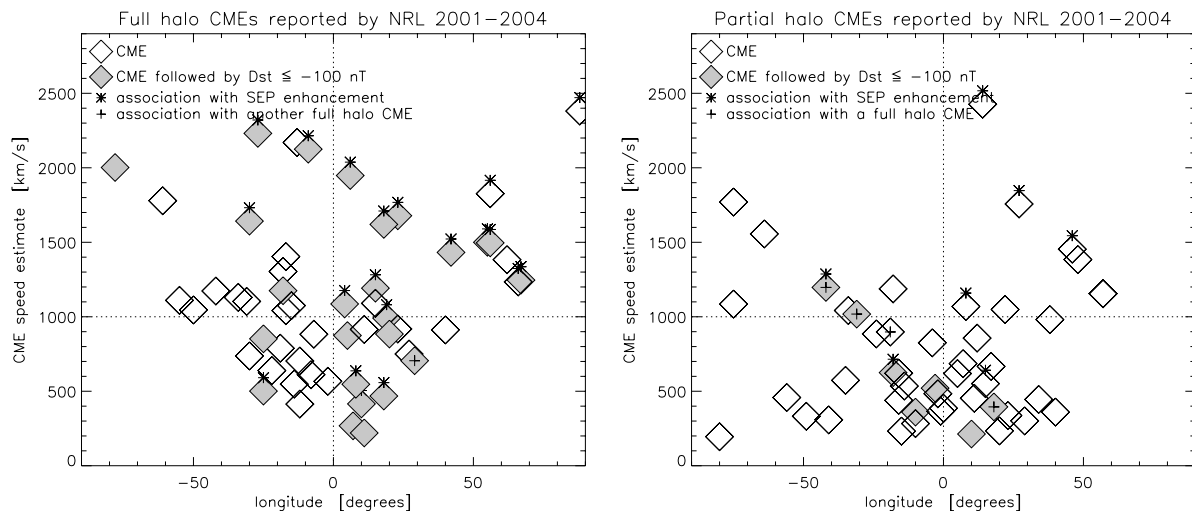
2.2. Solar eruptive events and geomagnetic storms

CMEs and strong geomagnetic storms are closely associated, as demonstrated by many studies of CME-storm relationships (e.g., Brueckner et al., 1998; Gosling et al., 1991; St. Cyr et al., 2000; Webb et al., 2000, 2001). In the study by St. Cyr et al. (2000) it was concluded that more than 80% of strong storms (defined by them as $Kp \geq 6$) were preceded by halo CMEs, but that more than half of all halo CMEs did not produce strong storms. The degree of association naturally depends on selection criteria and definitions of what constitute a strong geomagnetic storm. Nevertheless, the studies all agree that while most strong storms are caused by halo CMEs, many halo CMEs do not generate strong storms – it is not a one-to-one relationship. All halo CMEs are not equally geoeffective, even for identical classifications, e.g., “full halo CME” or “partial halo CME.” The geoeffectiveness of a CME also appear to depend on the background solar-wind in which it is propagating (Echer and Gonzalez, 2004). Despite this, the occurrence of a CME, and particularly a halo CME,

is presently the single most important indicator of upcoming geomagnetic disturbances.

Fig. 2 shows estimated CME speed and solar longitude for 101 front-sided halo CMEs reported by the NRL from March 2001 to April 2004. The CMEs are separated into “full halos” (left panel) and “partial halos” (right panel), and only those CMEs having an associated location determined from EIT observations are included. A CME is here defined as being associated with a magnetic storm if Dst falls below -100 nT in the time period between 24 and 96 h after CME onset. Such an association is indicated by a filled symbol in Fig. 2, while CMEs not followed by a strong magnetic storm are indicated by open symbols.

We first note that around 45% (25 out of 54) of all full halo CMEs reported by the NRL appear to generate a strong magnetic storm, largely confirming earlier studies (e.g., Cane et al., 2000; St. Cyr et al., 2000). Only around 15% (7 out of 47) of the partial halo CMEs show a similar association. This figure is further reduced to less than 10% (4 out of 47) when only considering partial halo CMEs that are not closely connected with a full halo CME. Apparently, the observation of a partial halo CME cannot be taken as an indication of an upcoming magnetic storm. Neither is the observation of a full halo CME by itself a particularly reliable indicator – many CMEs are not followed by a strong storm and the risk of a false alarm is high. It should, however, be noted that some of the full halo CMEs



Event	total number	followed by $Dst < -100$ nT	CME – storm association
full halo CME	54	25	46%
partial halo CME	47	7	15%
full halo CME + SEP	21	18	85%

Fig. 2. Estimated speed and heliographic longitude for halo CMEs classified and reported by the NRL based on LASCO/SOHO images. The CMEs associated with Dst below -100 nT are marked by grey shading, and CMEs associated with enhanced SEP signatures are marked by a star. The panel to the left show all CMEs from March 2001 to April 2004 classified as “full halos,” while the panel to the right show all CMEs classified as “partial halos.” We note that a large fraction of the full halo CMEs generating strong Dst disturbances also are associated with enhanced SEP signatures. Very few partial halo CMEs are associated with strong magnetic storms, unless they appear shortly before or after a full halo CME.

generate relatively strong geomagnetic disturbances at a level just below the strong-storm threshold utilized here, which means that moderate storms may still be considered. Nevertheless, there is obviously a need to improve the ability to discriminate the geoeffective CMEs from those less geoeffective.

Some of the CME properties, such as estimated CME speed and location of the CME on the solar disk, provide potentially useful information on the likelihood for a CME to generate a magnetic storm. However, as demonstrated in Fig. 2, these parameters are not particularly efficient as discriminators. In this study, we instead attempt to use SEP flux as a discriminator. In Fig. 2, all CMEs associated with enhanced SEP fluxes are indicated by a star on top of the CME symbol. The definition of enhanced SEP conditions used here is that the ≥ 10 MeV integrated flux should increase by more than a factor of 10 close to CME onset, or that the integrated flux should exceed 10 flux units following the CME. We note that there is a high degree of overlap between the full halo CMEs associated with enhanced SEP conditions and those followed by magnetic storms: of the 25 CMEs in the latter group and the 21 in the former group, 18 are in common, i.e., around 85% (18 out of 21) of all full halo CMEs associated with enhanced SEP conditions are followed by a strong magnetic storm. We therefore suggest that the flux of ≥ 10 MeV particles may be used days ahead as an indicator that an observed full halo CME is likely to generate a strong geomagnetic storm. Interestingly enough, a recent work by Smith et al. (2004) describes how the flux of 50 keV particles may be used to predict geomagnetic storms several hours ahead, i.e., with a lead time somewhere between the short and medium ranges as defined in this articles.

2.3. An example: November 22, 2001

In the evening of November 22, 2001, a full halo CME was observed by the LASCO instrument onboard the *SOHO* spacecraft (see Fig. 3 where the CME onset is indicated by a shaded diamond). The speed was estimated from the coronagraph images to more than 1200 km/s, and EUV enhancements in the low solar corona indicated the source region to be far out on the western side of the solar disk. Within minutes, a type II radio burst was observed, indicating the presence of a shock wave propagating in the solar corona with a velocity of around 900 km/s. At the same time, the SEP fluxes observed by the GOES satellites increased rapidly by several orders of magnitude – typical for an event that is magnetically well connected with the Earth – indicating the propagation of a strong shock in interplanetary space. Apparently, a substantial solar-wind disturbance could be expected to arrive some time during November 24, the exact time depending on which speed estimate we regard as most reliable. Warnings could be issued for a magnetic storm and after consideration of the daily and seasonal modulations of the locally observed dis-

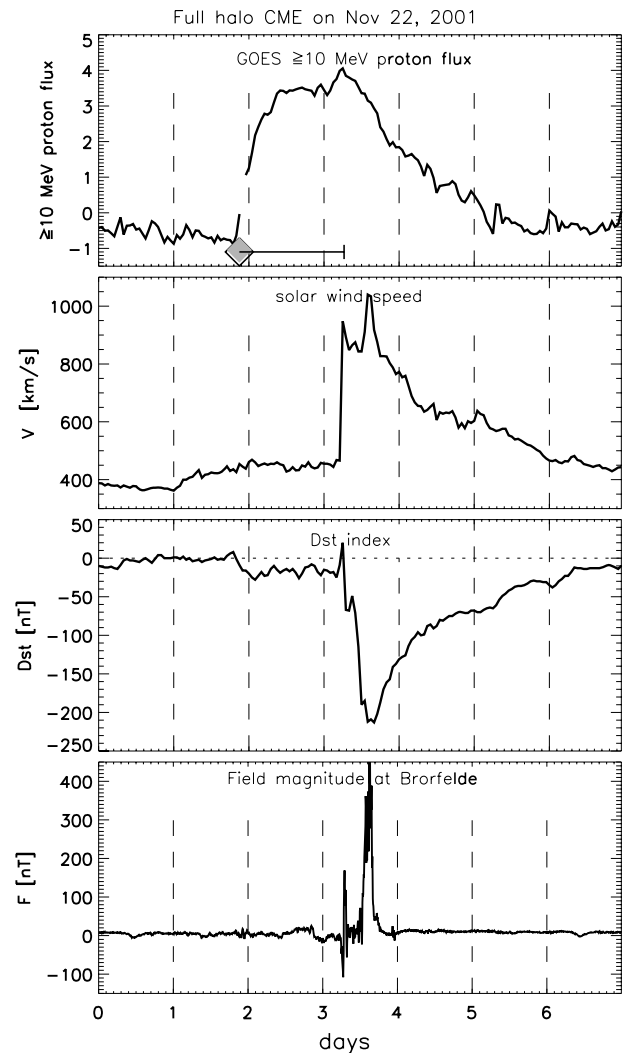


Fig. 3. An event where the overall relations between a halo CME, the SEP flux, and the resulting geomagnetic storm show a characteristic behaviour. Starting with a full halo CME (indicated by a shaded diamond in the top panel), and associated with strongly enhanced SEP fluxes, a propagating solar-wind disturbance causes a strong magnetic storm when passing by the Earth. During the main phase of the storm, very strong local disturbances are detected at the Brorfelde Observatory in Denmark.

turbances, the appropriate warnings could also be issued for the geomagnetic field at the Brorfelde Observatory in Denmark (bottom panel in Fig. 3).

3. Recurrent solar-wind structures

A substantial fraction of the weak and moderate geomagnetic disturbances exhibits a tendency to 27-day recurrence. In the absence of eruptive events on the Sun, the solar-wind is expected to be governed by large-scale quasi-static solar magnetic fields co-rotating with the Sun. Observations of the solar magnetic fields should in principle allow models of solar coronal expansion to be used for predictive purposes (Xuepu and Hoeksema, 1995; Wang et al., 1997). However, the observational constraints, our limited understanding of the solar-wind expansion processes, and the difficulties

involved in physical modelling, presently limit our ability to make model-based forecasts. Nevertheless, on-going attempts to use solar-wind models in an operational setting prove them to be potentially useful.

3.1. Observations and real time data

Several ground based solar observatories – the Wilcox Solar Observatory (WSO) at Stanford, the Mount Wilson Solar Observatory (MWO), and the National Solar Observatory (NSO) at Kitt Peak – routinely produce solar magnetograms, i.e., low-resolution synoptic maps of the line-of-sight component of the photospheric magnetic fields. These maps are extended outward by means of a potential field model to give the distribution of radial magnetic field lines at the *source surface*, normally defined as a spherical surface at 2–3 solar radii. The conditions thus derived should, however, only be regarded as giving a rough picture of the true conditions at the base of the solar-wind: the daily photospheric fields are only observed in a limited region close to central meridian (Hoeksema, 1984) and each magnetogram is derived from many daily observations of solar magnetic fields that in reality may evolve quite substantially during a solar rotation. It was also recently shown by Poduval and Zhao (2004) that the derived coronal magnetic structures depend sensitively on the type of potential-field model that is used. Most of the time, solar magnetograms are

available in near-real time on a daily basis for use as input to solar-wind models.

The solar-wind and the interplanetary magnetic field (IMF) are continuously monitored from the Sun–Earth libration point L_1 by the ACE and SOHO spacecraft. These data are transmitted to Earth and distributed in real time through NOAA’s Space Environment Center.

3.2. Solar wind streams and geomagnetic storms

Fig. 4 shows a 7-month period during the latest solar minimum in 1995, when the solar-wind was governed by large-scale structures co-rotating with the Sun. Significant eruptive events on the Sun was largely absent during this period.

We find several moderate magnetic storms, defined by $Dst < -50$ nT, and one major magnetic storm, defined by $Dst < -100$ nT. There is a clear tendency for the magnetic storms to be associated with rapid increases from a low solar-wind speed, around 300–400 km/s, to a high solar-wind speed, around 550–800 km/s. At these low speed/high speed interfaces, or *stream interfaces*, the solar-wind plasma is being compressed, leading to an increased solar-wind density and a strengthening of the IMF. Normally, we also find *magnetic sector boundary* crossings in association with the stream interfaces. The geomagnetic disturbances found near these very distinct solar-wind features are caused by the high solar-wind speeds and the stronger-than-average

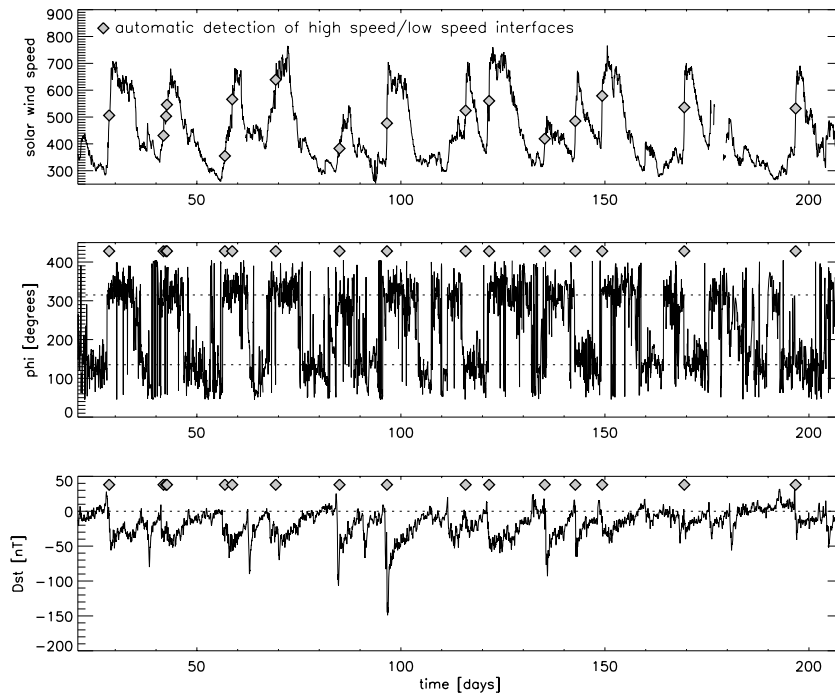


Fig. 4. A 7-month period during the latest solar minimum in 1995 when the solar-wind was governed by large-scale structures co-rotating with the Sun. The figure shows the solar-wind speed (upper panel), the direction of the interplanetary magnetic field in the ecliptic plane (middle panel), and the geomagnetic disturbances as measured by the Dst index (lower panel). Filled symbols indicate detection of low speed/high speed interfaces by a fully automatic procedure that can be applied both to observed and modelled solar-wind data.

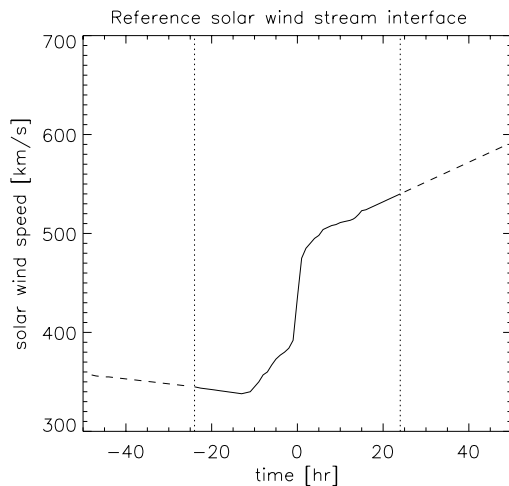


Fig. 5. The reference solar-wind speed profile obtained from a superposition of 30 well-defined solar-wind stream interfaces centered on the maximum time derivative. Large co-variances between this time series and the observed solar-wind time series indicate the occurrence of stream interfaces, as shown in the upper panel of Fig. 4. The application to modelled, instead of observed, solar-wind data allow forecasts of stream interfaces to be made days ahead, the accuracy depending on the solar-wind models.

IMF magnitudes, in combination with a very irregular IMF which often, though not always, leads to short periods of a large out-of-ecliptic IMF component. If southward directed, a moderate magnetic storm is likely to follow.

The filled symbols in Fig. 4 indicate stream interfaces as detected by a fully automatic procedure based on a relatively simple cross-correlation technique. From a few years of data during the latest solar minimum, around 30 well-defined stream interfaces were selected. These were superposed to produce an average solar-wind speed profile consisting of the central 48 h centered on the maximum time derivative (Fig. 5). After normalization to zero mean and the same standard deviation as the reference velocity profile, the 7 months shown in Fig. 4 were scanned for local maxima of the covariance between the observed time series and the reference time series. The local maxima having a covariance above 0.5 were selected as candidate stream interfaces, shown as diamonds in Fig. 4.

It is interesting to note, from the lower panel in Fig. 4, the high degree of association between these automatically detected features and the moderate magnetic storms. The automatic procedure could equally well be applied to a modelled solar-wind time series to find the corresponding modelled solar-wind features. As described below, such models do exist and at least two of them are currently used in an operational, real-time mode.

3.3. Solar wind modelling in near-real time

As described in Section 1, fundamental limitations prevent medium-range predictions of the out-of-ecliptic IMF component B_Z . This fact impose severe restrictions on

the medium-range forecasts of geomagnetic activity. We cannot simply feed geomagnetic-forecast models with the unfiltered output from a solar-wind model. However, it is important to make a clear distinction between solar-wind parameters that are not predictable, and solar-wind parameters that are – at least in principle – predictable. Due to much larger temporal and spatial scales, the velocity, the IMF magnitude, the polarity of the radial IMF component B_X , and the boundaries that separate regions of interplanetary space in which different conditions prevail, are predictable.

Solar wind stream interfaces, such as those shown in Fig. 4, belong to this group of predictable parameters. If the solar-wind predictions based on observations of the Sun are sufficiently accurate, the association between stream interfaces and moderate storms described in Section 3.2 could be utilized to make geomagnetic forecasts on a medium-range time scale. In such a prediction scheme, a solar-wind model provides a deterministic prediction of the stream interfaces which are likely to generate moderate storms, essentially introducing a deterministic element into the probabilistic forecast schemes. This has been proposed by many authors (e.g., Akasofu and Fry, 1986; Dryer et al., 1986; Detman and Vassiliadis, 1997). More recently, and in a more elaborated form, it was brought forward by McPherron and Siscoe (2003).

In the scientific literature, there are several models described for computing the near-Earth solar-wind conditions from observations of solar photospheric magnetic fields and derived coronal magnetic fields. Data based models (Wang and Sheeley, 1990; Wang et al., 1997; Wintoft and Lundstedt, 1997) take the derived coronal magnetic fields as the starting point to compute the solar-wind speed and radial IMF component at Earth's orbit through static functional relationships. Recent developments of one of these models also allow for a certain degree of stream interaction (Arge et al., 2003). This model, also referred as the Wang–Sheeley–Arge (WSA) model, seems to be in a state of development with the aim to replace empirical relations with physics based modelling.

The Hakamada–Akasofu–Fry (HAF) model (Fry et al., 2001) start off with the same observational data, but use them to define the inner boundary conditions of a physical model: a 3D “modified kinematic” model that projects the flow of solar-wind from the inhomogeneous source surface out into interplanetary space, automatically adjusting for stream–stream interactions. If the speed difference across a stream interface is large enough, a shock may form.

Both the WSA and the HAF models are currently running in a real-time, operational mode, and the results are automatically disseminated to the user community through Internet. The practical usefulness of these solar-wind models for the purpose of predicting geomagnetic activity is currently limited by significant errors in the time of arrival of potentially geoeffective solar-wind features: 12 h is a

typical error, but it is not uncommon to find deviations around 1 day or even larger. These errors can only partly be explained by limitations in the solar-wind models themselves. As pointed out in Section 3.1, the boundary conditions at the source surface are also uncertain due to fundamental observational and computational limitations. Nevertheless, despite these practical restrictions, we find several occasions when the solar-wind models, in combination with the feature detection technique described above, contribute to more accurate medium-range forecasts of moderate storms. Geomagnetic storms during last few years have largely been generated by solar eruptive events, but as we now approach the next solar minimum recurrent structures will become more important, giving us the opportunity to test the use of solar-wind models more rigorously.

4. Discussion

In this paper, we discuss presently used concepts and some new ideas for fully automatic provision of geomagnetic activity forecasts hours to days ahead. This time span, which we refer to as *medium-range*, is loosely defined by the propagation of solar-wind disturbances from Sun to Earth. We have also referred to forecasts an hour ahead as *short-range* forecasts. This nomenclature deviates from that often used, e.g., by Joselyn (1995), but agrees with that expressed by McPherron and Siscoe (2004).

The relations between solar eruptive events and geomagnetic storms described in Section 2 are already extensively used by operational space weather forecast services. Much of these developments have taken place since the launch of the SOHO spacecraft in December 1995. The use of physics-based modelling described in Section 3, and the implementation of space weather forecast services more similar to terrestrial weather forecasting on a conceptual level, have not been equally well explored. It is the intention of the current development project to do so, and to combine the two modes of prediction – that based on solar eruptive events, and that based on quasi-static structures co-rotating with the Sun – to produce fully automatic geomagnetic forecasts for a wide range of solar-activity conditions.

Acknowledgments

This work was done as a part of the ESA *Space Weather Applications Pilot Project*, under ESTEC Contract 16983/03/NL/LvH. The LASCO team at the Naval Research Laboratory are gratefully acknowledged for their efforts at prompt identification of potentially geoeffective halo CMEs. Output from the Wang–Sheeley–Arge (WSA) model are obtained from NOAA's Space Environment Center in Boulder, and data from the Hakamada–Akasofu–Fry (HAF) model are provided by the Geophysical Institute at the University of Alaska. Nick Arge and Murray Dryer are acknowledged for providing us with real-time access to these data.

References

- Akasofu, S.-I., Fry, C.F. A first generation numerical geomagnetic storm prediction scheme. *Planet Space Sci.* 34, 77–92, 1986.
- Arge, C.N., Odstrcil, D., Pizzo, V.C., Meyer, L.R. Improved method for specifying solar-wind speed near the Sun, in: Velli, M., Bruno, R., Malara, F. (Eds.), *Solar Wind Ten: Proceedings of the Tenth International Solar Wind Conference*, 2003.
- Bartels, J. Terrestrial magnetic activity and its relations to solar phenomena. *J. Geophys. Res.* 37, 1–52, 1932.
- Berghmans, D., Foing, B.H., Fleck, B. Automated detection of CMEs in LASCO data, in: *Proceedings of the SOHO-11 Workshop*, Davos, 2001, ESA SP-508, 2002.
- Bruelckner, G.E., Delaboudiniere, J.-P., Howard, R.A., Paswaters, S.E., St.Cyr, O.C., Schwenn, R., Lamy, P., Simnett, G.M., Thompson, B., Wang, D. Geomagnetic storms caused by coronal mass ejections (CMEs): March 1986 through June 1997. *Geophys. Res. Lett.* 25, 3019–3022, 1998.
- Cane, H.V., Richardson, I.G., St. Cyr, O.C. Coronal mass ejections, interplanetary ejecta and geomagnetic storms. *Geophys. Res. Lett.* 27, 3591–3594, 2000.
- Detman, T.R., Cross validation comparisons of autonomous *Ap* Predictions, in: *Proceedings of the Workshop on the Evaluation of Space Weather Forecasts*, NOAA, Boulder, Colorado, pp. 149–160, 1996.
- Detman, T.R., Vassiliadis, D. Review of techniques for magnetic storm forecasting, in: *Magnetic storms*, AGU Geophysical Monograph 98, AGU, Washington, MD, pp. 253–266, 1997.
- Dryer, M., Akasofu, S.-I., Kroehl, H.W., Sagalyn, R., Wu, S.T., Tascione, T.F., Kamide, Y. The solar/interplanetary/ionosphere/connection: a strategy for prediction of geomagnetic storms. *Adv. Astro. Sci.*, 58, 1986.
- Echer, E., Gonzalez, W.D. Geoeffectiveness of interplanetary shocks, magnetic clouds, sector boundary crossings and their combined occurrence. *Geophys. Res. Lett.*, 31, doi:10.1029/2003GL019199, 2004.
- Fry, C.D., Sun, W., Deehr, C.S., Dryer, M., Smith, Z., Akasofu, S.-I., Tokumaru, M., Kojima, M. Improvements to the HAF solar-wind model for space weather prediction. *J. Geophys. Res.* 106, 20985–21001, 2001.
- Gleisner, H., Lundstedt, H. A neural network-based local model for prediction of geomagnetic disturbances. *J. Geophys. Res.* 106, 8425–8434, 2001.
- Gosling, J.T., McComas, D.J., Phillips, J.L., Bame, S.J. Geomagnetic activity associated with earth passage of interplanetary shock disturbances and coronal mass ejections. *J. Geophys. Res.* 96, 7831, 1991.
- Hoeksema, J.T., Structure and evolution of the large scale solar and heliospheric magnetic fields, PhD Thesis, Stanford Univ., Palo Alto, California, 1984.
- Joselyn, J.A. Geomagnetic activity forecasting: the state of the art. *Rev. Geophys.* 33, 383–401, 1995.
- McPherron, R.L., Siscoe, G. Probabilistic forecasting of geomagnetic indices using solar-wind “air mass” analysis. *Space Weather* 1, 3–14, doi:10.1029/2003SW000003, 2003.
- McPherron, R.L., Siscoe, G.L. Probabilistic forecasting of geomagnetic indices using solar-wind air mass analysis. *Space Weather* 2, S01001, doi:10.1029/2003SW000003, 2004.
- O'Brien, T.P., McPherron, R.L. Forecasting the ring current index Dst in real time. *J. Atmos. Solar-Terr. Phys.* 62, 1295–1299, 2000.
- Poduval, B., Zhao, X.P. Discrepancies in the prediction of solar-wind using potential field source surface model: an investigation of possible sources. *J. Geophys. Res.*, 109, doi:10.1029/2004JA010384, 2004.
- Sargent, H.H. The 27-day recurrence index, in: Kamide, Y., Slavin, J.A. (Eds.), *Solar Wind-Magnetosphere Coupling*, pp. 143–154, 1986.
- Smith, Z., Murtagh, W., Smithro, C. Relationships between solar-wind low-energy energetic ion enhancements and large geomagnetic storms. *J. Geophys. Res.*, 109, doi:10.1029/2003JA010044, 2004.

- St. Cyr, O.C., Howard, R.A., Sheeley Jr., N.R., Plunkett, S.P., Michels, D.J., Paswaters, S.E., Koomen, M.J., Simnett, G.M., Thompson, B.J., Gurman, J.B., Schwenn, R., Webb, D.F., Hildner, E., Lamy, P.L. Properties of coronal mass ejections: SOHO LASCO observations from January 1996 to June 1998. *J. Geophys. Res.* 105, 18169–18185, 2000.
- Thomson, A.W.P. Non-linear predictions of A_p by activity class and numerical value. *Pure Appl. Geophys.* 146, 163–193, 1996.
- Valdivia, J.A., Vassiliadis, D., Klimas, A.J., Sharma, A.S. The spatio-temporal activity of magnetic storms. *J. Geophys. Res.* 104, 12239–12250, 1999.
- Wang, Y.M., Sheeley, N.R. Solar wind speed and coronal flux tube expansion. *Astrophys. J.* 355, 726–732, 1990.
- Wang, Y.M., Sheeley, N.R., Phillips, J.L., Goldstein, B.E. Solar wind stream interactions and the wind speed-expansion factor relationship. *Astrophys. J. Lett.* 488, L51–L54, 1997.
- Webb, D.F., Cliver, E.W., Crooker, N.U., St. Cyr, O.C., Thompson, B.J. Relationship of halo coronal mass ejections, magnetic clouds, and magnetic storms. *J. Geophys. Res.* 105, 7491–7508, 2000.
- Webb, D.F., Crooker, N.U., Plunkett, S.P., St. Cyr, O.C. The solar sources of geoeffective structures, in: *Space Weather*, AGU Geophysical Monograph 125, AGU, Washington, MD, pp. 123–141, 2001.
- Wintoft, P., Lundstedt, H. Prediction of daily average solar-wind velocity from solar magnetic field observations using hybrid intelligent systems. *Phys. Chem Earth* 22, 617–622, 1997.
- Xuepu, Z., Hoeksema, J.T. Prediction of the interplanetary magnetic field strength. *J. Geophys. Res.* 100, 19–33, 1995.
- Zhao, X.-P., Hoeksema, J.T. Is the geoeffectiveness of the January 6, 1997, CME predictable from solar observations? *Geophys. Res. Lett.* 24, 2965–2968, 1997.